**SUPPLEMENTARY MATERIAL.**

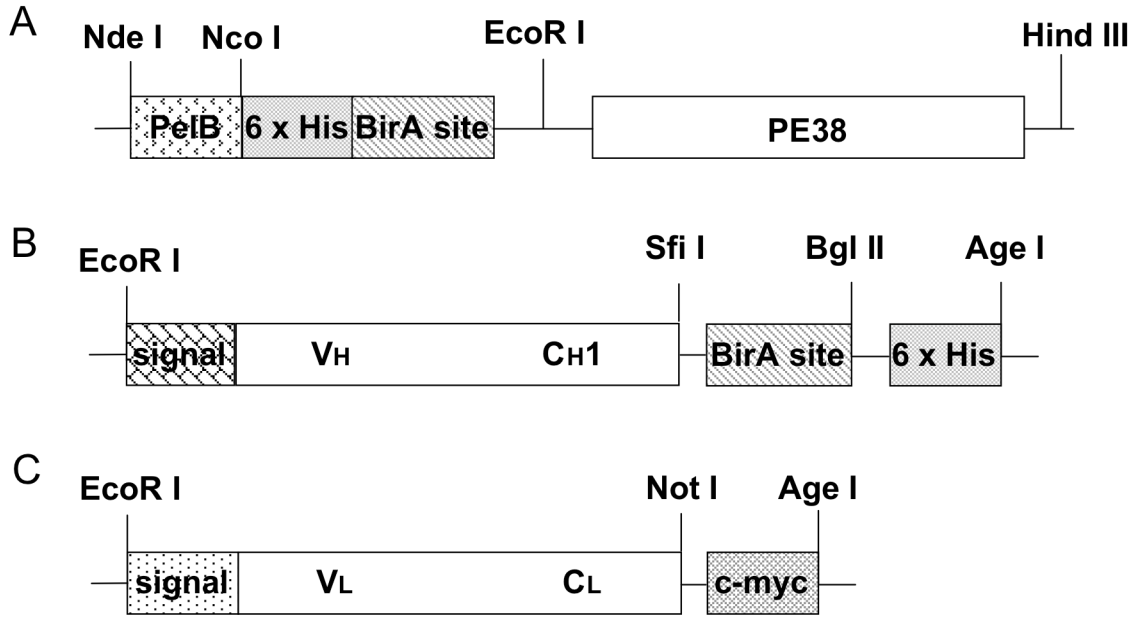


**Figure S1. Construction of plasmids expressing PE38 toxin subunit (A) and 25-D1.16 Fd fragment (B) and the light chain (C).** See Material and Methods for details.

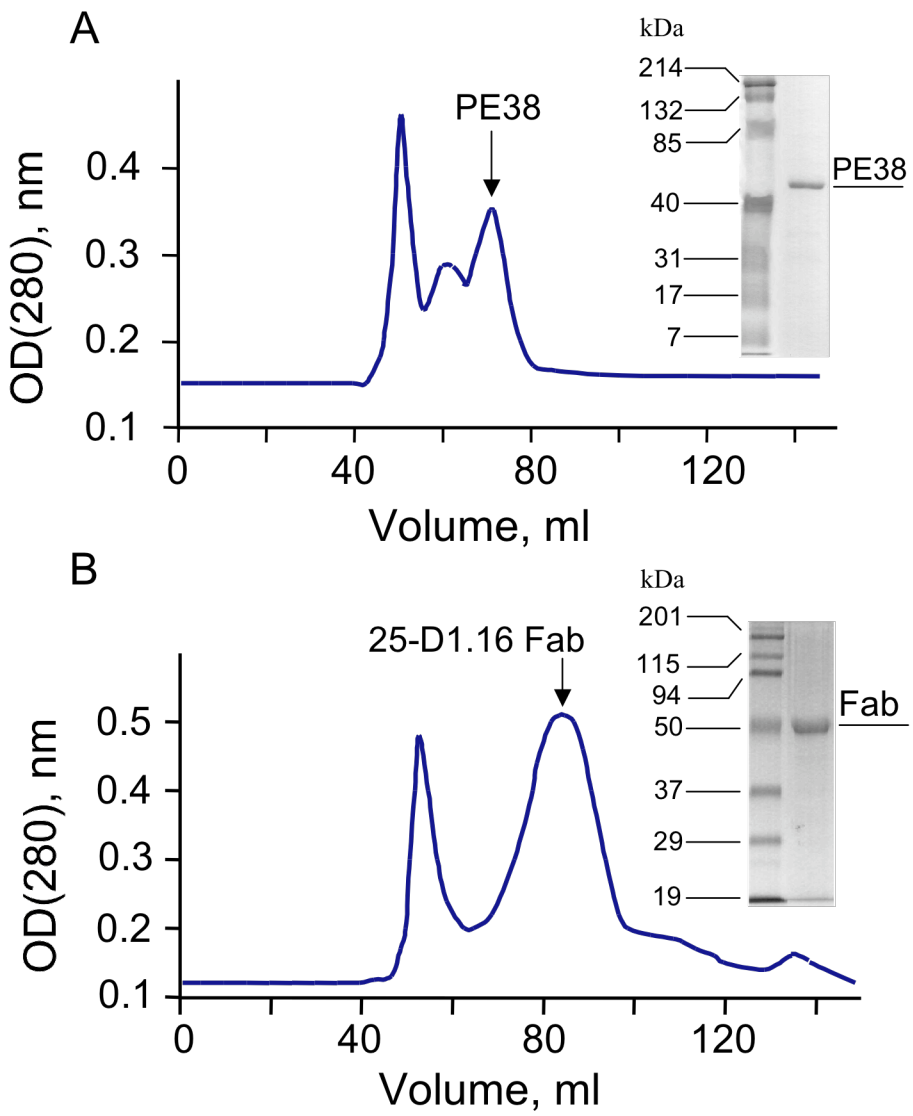


**Figure S2. Purification of recombinant 25-D.1-16 (A) and PE38 (B) proteins.**
Both recombinant proteins were initially purified on NiNTA column. Material eluted from NiNTA column was further purified by gel-filtration on Sepharcryl S-200 column to remove aggregated protein. The gel-filtration profiles for 25-D1.16 Fab and PE38 are shown. An arrow designates peak containing protein free of aggregates. Purity of aggregate free material was confirmed by PAGE SDS analysis. See Material and Methods for details.

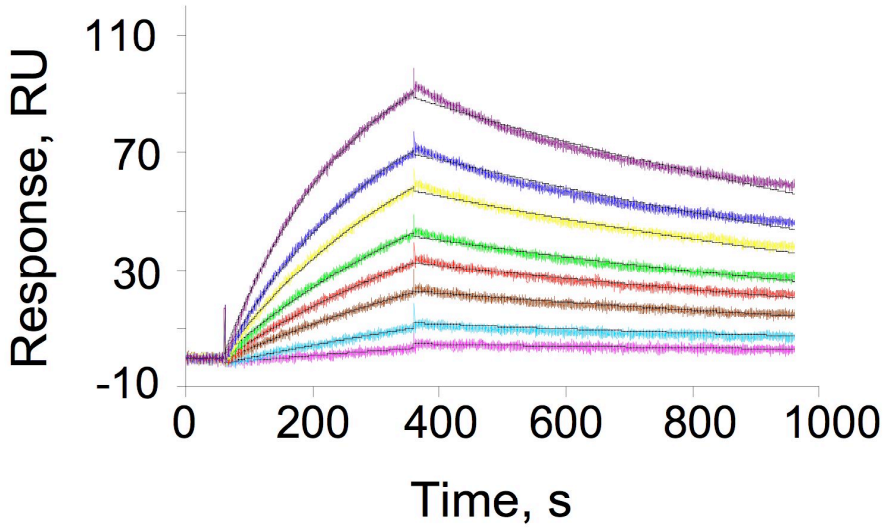


| 25-D1.16 Fab | $k_{ass}$, $M^{-1}s^{-1}$ | $k_{diss}$, $s^{-1}$ | $K_{eq.ass}$, $M^{-1}$ | $K_{eq.diss}$, M |
|---|---|---|---|---|
| Native | $2.95x10^{4}$ | $7.30x10^{-3}$ | $4.04x10^{6}$ | $2.48x10^{-7}$ |
| Recombinant | $3.5x10^{4}$ | $7.22x10^{-3}$ | $4.85x10^{6}$ | $2.06x10^{-7}$ |
| | | | | |

**Figure S3. Interaction of soluble pOV8-$K^b$ with recombinant 25-D1.16 Fab fragment immobilized on a biosensor surface**

Sensograms show association and dissociation phases of the binding of soluble pOV8-$K^b$ complex at various concentrations to recombinant 25-D1.16 Fab immobilized on a biosensor surface 400 Response Units (R.U.). The experiments were performed essentially as previously described (17). The Table show binding parameters for the interaction of soluble pOV8-$K^b$ with either native (17) or recombinant 25-D1.16 Fab.

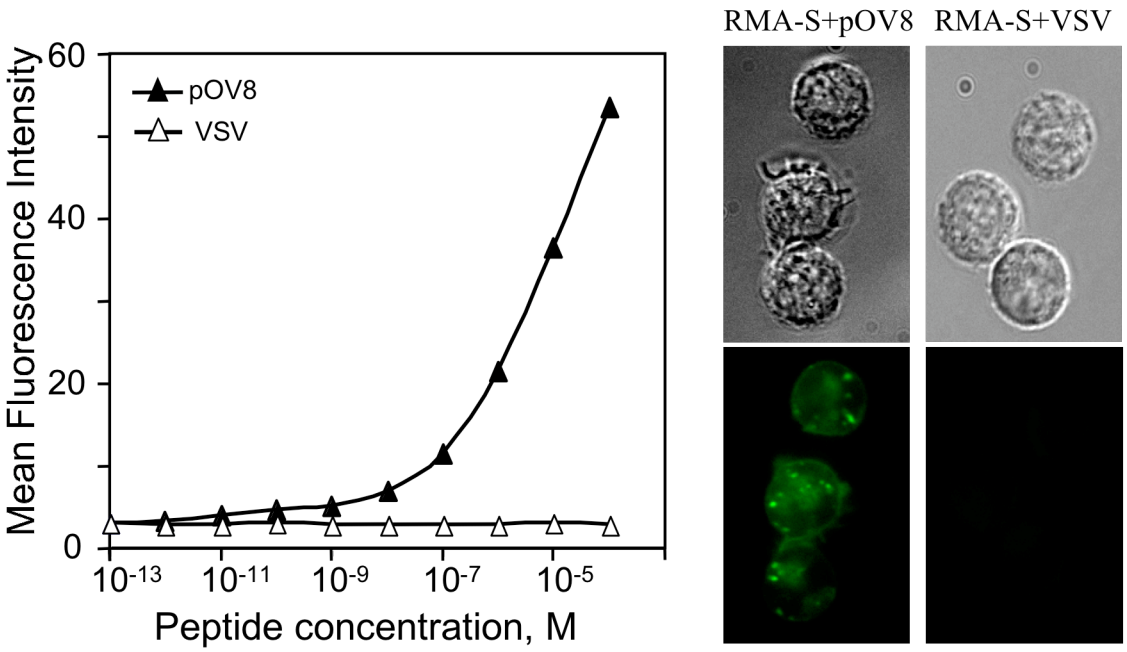


**Figure S4. Fluorescent-labeled 25-D1.16 tetramer specifically binds to RMA-S cells sensitized with pOV8 but not with VSV peptide.**

LEFT: The dependence of mean fluorescence intensity (MFI) of cell-bound 25-D1.16 tetramer versus peptide concentration used to sensitize RMA-S cells.

RIGHT: IRM (top) and fluorescent (bottom) images of RMA-S cells sensitized with either pOV8 or VSV peptides at saturated concentrations. Specific binding of 25-D1.16 tetramer at 37ºC resulted in rapid endocytose as evident from the intracellular staining. The tetramer binding at 4ºC produced mostly membrane staining (not shown).

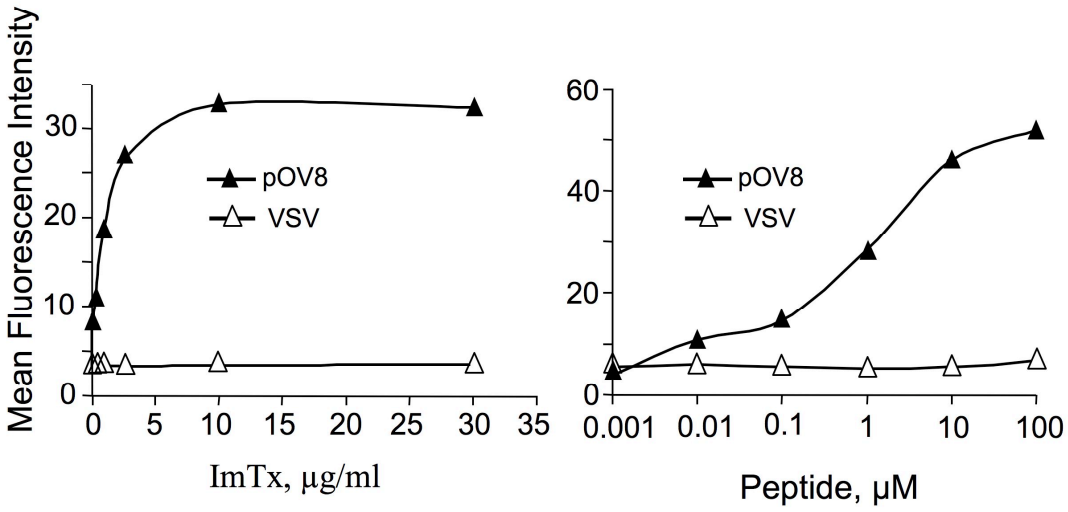


**Figure S5. ImTx specifically binds to RMA-S cells sensitized with pOV8 peptide but not with VSV peptide.**

LEFT: The dependence of MFI versus concentration of fluorescent-labeled ImTx added to the extracellular medium of RMA-S cells sensitized with either pOV8 or VSV peptides at saturated concentrations.

RIGHT: MFI of fluorescent-labeled ImTx bound to RMA-S cells as a function of peptide concentration is shown. The cells were sensitized with either pOV8 or VSV at indicated concentrations.

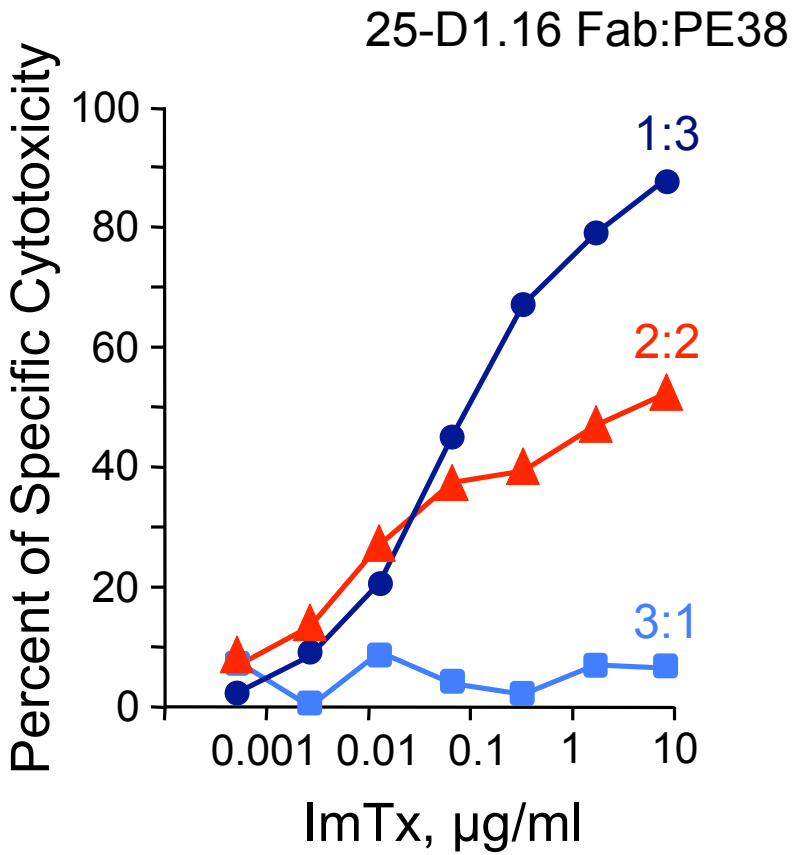


**Figure S6. Effectiveness of cytotoxic activity of ImTx against pOV8-sensitized target cells depends on the ratio of recombinant 25-D1.16 Fab and PE38 in the ImTx.**

Recombinant biotinylated 25-D1.16 Fab fragment and PE38 toxin were combined at various ratios as described in Material and Methods. The toxicity of the ImTx containing indicated ratios of the Fab/PE38 against H-2K$^{b+}$ RMA-S cells loaded with pOV8 peptide at 3 μM was tested using MTS assay (Promega) as described in Material and Methods. The 2:2 rather than 1:1 ratio is shown to emphasize that all Streptavidin binding sites were occupied, i.e., two of them having the 25-D1.16 Fab and two others bearing the PE38 toxin subunit on average. Each concentration of the toxin was tested in triplicate.

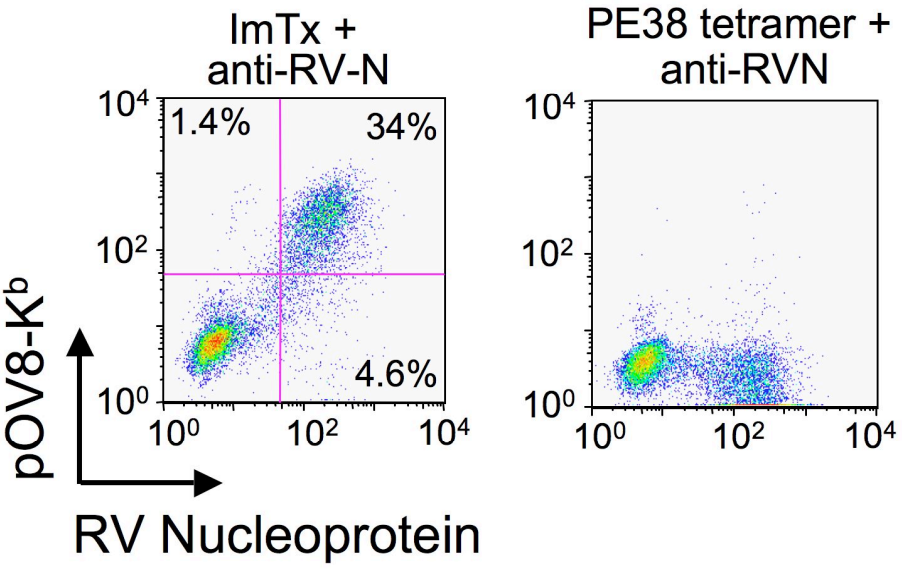


**Figure S7. Double staining of RV-pOV8-infected IL4 cells with fluorescent-labeled ImTx or labeled PE38 tetramer and anti-RV-N antibodies.**
All cells positive for staining with anti-RV-N antibody were also stained with ImTx but not with PE38 tetramer (see Material and Methods for details on double staining protocol).